# In Vivo, Villin Is Required for $Ca^{2+}$-dependent F-actin Disruption in Intestinal Brush Borders

**Evelyne Ferrary,* Michel Cohen-Tannoudji,‡ Gérard Pehau-Arnaudet,* Alexandre Lapillonne,* Rafika Athman,* Tereza Ruiz,* Lilia Boulouha,*§ Fatima El Marjou,* Anne Doye,* Jean-Jacques Fontaine,§ Claude Antony,* Charles Babinet,‡ Daniel Louvard,* Frédéric Jaisser,* and Sylvie Robine***

*Institut Curie, UMR 144, 75248 Paris, France; ‡Unité de Biologie du Développement, Centre National de la Recherche Scientifique, URA 1960, Institut Pasteur, 75015 Paris, France; and §Ecole Nationale Vétérinaire d'Alfort, 94700 Maisons-Alfort, France

*Abstract.* Villin is an actin-binding protein localized in intestinal and kidney brush borders. In vitro, villin has been demonstrated to bundle and sever F-actin in a $Ca^{2+}$-dependent manner. We generated knockout mice to study the role of villin in vivo. In villin-null mice, no noticeable changes were observed in the ultrastructure of the microvilli or in the localization and expression of the actin-binding and membrane proteins of the intestine. Interestingly, the response to elevated intracellular $Ca^{2+}$ differed significantly between mutant and normal mice. In wild-type animals, isolated brush borders were disrupted by the addition of $Ca^{2+}$, whereas $Ca^{2+}$ had no effect in villin-null isolates. Moreover, increase in intracellular $Ca^{2+}$ by serosal carbachol or mucosal $Ca^{2+}$ ionophore A23187 application abolished the F-actin labeling only in the brush border of wild-type animals. This F-actin disruption was also observed in physiological fasting/refeeding experiments. Oral administration of dextran sulfate sodium, an agent that causes colonic epithelial injury, induced large mucosal lesions resulting in a higher death probability in mice lacking villin, 36 ± 9.6%, compared with wild-type mice, 70 ± 8.8%, at day 13. These results suggest that in vivo, villin is not necessary for the bundling of F-actin microfilaments, whereas it is necessary for the reorganization elicited by various signals. We postulate that this property might be involved in cellular plasticity related to cell injury.

Key words: villin knockout • intestine • actin-binding proteins • microvilli • mouse



INTESTINAL epithelial cells have two distinct membrane domains, the apical and basolateral surfaces. The apical surface exhibits numerous digitations that form the highly organized brush border. During the last 20 years, most of the microvillar structural proteins have been isolated and their primary sequences determined. More recently, their biological functions have been evaluated by in vitro and cell culture experiments. The challenge now is to determine their in vivo functions, the roles they play in the assembly of the brush border during terminal differentiation, and the molecular basis of the cytoskeleton–protein interactions. Actin-binding proteins have been reported to play a major role in the formation of the microvillus core bundle (Glenney et al., 1980; Mooseker et al., 1980; Matsudaira and Burgess, 1982; Coluccio and Bretscher, 1989). These proteins are known to modulate the dynamics of the actin cytoskeleton by mediating changes of the state of actin polymerization and the spatial arrangement of actin protofilaments. Among the actin-binding proteins, we have chosen villin as a model protein to gain insight into the mechanisms by which actin and its associated proteins contribute to morphological processes in the intestinal epithelial cells.

Villin is a monomeric 92.5-kD protein that is expressed mainly in absorptive epithelial cells such as those of small and large intestine and proximal tubule in kidney (Bretscher and Weber, 1979; Matsudaira and Burgess, 1979; Robine et al., 1985). Villin is a multidomain protein composed of two very similar domains repeated in tandem, each of ~44 kD forming the core of the protein, and a COOH-terminal domain of 8.5 kD called the head piece (Glenney and Weber, 1981; Arpin et al., 1988; Bazari et

F. Jaisser and S. Robine contributed equally to this paper. This work has been presented in part at the 6th International Congress on Cell Biology in San Francisco on 7–11 December 1996. Portions of this work have appeared in abstract form (1996. *Mol. Biol. Cell.* 7[Suppl.]:2*a* and 542*a*).

E. Ferrary's present address is Institut Nationale de la Santé et Recherche Médicale, U426, Faculté Xavier Bichat, 75018 Paris, France.

F. Jaisser's present address is Institut Nationale de la Santé et Recherche Médicale, U428, Faculté Xavier Bichat, 75018 Paris, France.

Address correspondence to Sylvie Robine, UMR 144, Laboratoire de Morphogénèse et Signalisation Cellulaires, Institut Curie, 26, rue d'Ulm, 75248 Paris cedex 05, France. Tel.: 33-1-42-34-63-62. Fax: 33-1-42-34-63-77. E-mail: Sylvie.Robine@curie.fr

al., 1988). Villin belongs to a large family of $Ca^{2+}$-regulated actin-binding proteins which share structural and functional similarities. The related proteins are gelsolin (Kwiatkowski et al., 1986), scinderin (Marcu et al., 1994), adseverin (Bader et al., 1986), supervillin (Pestonjamasp et al., 1997), dematin (Rana et al., 1993), and advillin (Marks et al., 1998) in higher eukaryotes, as well as severin and fragmin in lower eukaryotes (Ampe and Vandekerckhov, 1987; André et al., 1988) (for reviews see Mooseker, 1985, and Friederich et al., 1990). The primary structure of these proteins presents sequence homology within the sixfold repeated domain and/or the seventh COOH-terminal domain.

The bundling activity of villin was first assessed in transfection experiments in cultured cells: villin induced the growth of microvilli on the dorsal faces of fibroblastic CV1 cells, with the reorganization of the underlying actin cytoskeleton. Villin core (lacking the head piece domain) was unable to promote these morphological modifications (Friederich et al., 1989, 1992). Furthermore, using an antisense RNA strategy in human intestinal CaCo2 cells, permanent downregulation of the endogenous villin messenger dramatically affected brush border assembly. This effect was reversed by transfection with a cDNA encoding a partial-sense villin RNA (Costa de Beauregard et al., 1995). Together, these results suggest that villin should play a role in brush border assembly by establishing and/or maintaining microvillar structures.

The severing activity of villin has been demonstrated in solution, in the presence of high concentration of $Ca^{2+}$ ($10^{-4}$ M) (Bretscher and Weber, 1980). Moreover, this concentration of $Ca^{2+}$ induced vesiculation of intestinal brush border microvilli and the breakdown of the actin core bundle (Burgess and Prum, 1982). The severing activity of villin resides in the $NH_2$-terminal half of the core, a region similar to that comprising the severing properties of gelsolin, although the severing activity of villin is highly regulated by the $Ca^{2+}$ concentration, whereas that of gelsolin is not (Northrop et al., 1986). The villin severing activity has been proposed to take place under certain physiological conditions, such as bacterial infection or responses to fasting and feeding, depending on the level of intracellular $Ca^{2+}$ (Misch et al., 1980; Glenney and Glenney, 1985; Knutton et al., 1993).

The purpose of this study was to investigate, in vivo, the bundling and the severing of actin microfilaments in the absence of villin. In the villin-null mice the gross assembly of the intestinal microvilli was not affected, and no noticeable change in the localization and expression of the actin-binding proteins was observed. In contrast, villin appears to be a major protein able to control the $Ca^{2+}$-dependent actin fragmentation in physiological or pharmacological conditions. These results suggest that, in vivo, the bundling activity of villin is dispensable, i.e., redundant and/or compensated, whereas the severing activity is not. Finally, we show that villin is required for survival in experimental colitis caused by the oral administration of dextran sulfate sodium (DSS).[1] Hence, these data lead us to propose a role for villin in cell remodeling controlled by cortical actin in stressed animals.

1. *Abbreviations used in this paper:* BBMI, brush border myosin I; DSS, dextran sulfate sodium; ES, embryonic stem.

## Materials and Methods

### Construction of Targeting Vectors

A 6.5-kb BamHI fragment was isolated from a λDASHII phage containing 16 kb of the mouse *villin* gene (kindly furnished by G. Tremp, Rhône Poulenc RORER) and subcloned in pBS/KS+ (Stratagene). The *neomycin* resistance gene (pMC1neo; Stratagene) was introduced in a unique KpnI site in *villin exon* 2. This disrupts the open frame reading of the *villin* gene. The neo cassette was placed in the reverse transcriptional orientation compared with the *villin* gene. The construct contained 3.5 and 3 kb of homology regions, 5′ and 3′, respectively. In addition, the Herpes simplex virus (HSV) thymidine kinase expression cassette (Thomas and Capecchi, 1987) was inserted in the unique ClaI site flanking the 5′ end of the construct. This resulted in the p*villin neo* targeting construct.

### ES Cell Culture and Generation of Chimeric Mice

The CK35 ES cell line (Kress et al., 1998) was cultured in DMEM (GIBCO BRL) supplemented by 1 mM Na-Pyruvate, 15% FCS (Techgen International), 1,000 U/ml LIF (ESGRO; GIBCO BRL), and 50 mM β-mercaptoethanol (GIBCO BRL) as described (Cohen-Tannoudji et al., 1998). $2 \times 10^7$ CK35 ES cells were electroporated with 20 μg of the p*villin neo* targeting construct linearized in the plasmid backbone (PvuI site). G418 (300 μg/ml) was added 36 h after plating for 12 d. Gancyclovir (2 μM) was added with G418 from day 2 to day 8 of selection. The G418-resistant clones were isolated and their genotype analyzed by Southern blot.

Chimeric mice were generated by microinjection of the targeted ES cells into C57Bl6 blastocysts as described (Bradley, 1987). Crosses between chimeric male and C57Bl6/DBA2 females generated heterozygous animals which were then intercrossed to generate homozygous animals. The following experiments were performed in sibling villin-null mice and wild-type animals with the same mixed genetic background.

### Sampling and Preparation of the Tissues

The mice were killed with an intraperitoneal injection of a lethal dose of pentobarbital, or anesthetized when necessary with a 50 μl/10 g body wt of a mixture of 750 μl xylazine (Rompun™ 2%; Bayer), 6 ml Imalgene™ (Rhône Merieux), and 300 μl Flunitrazepan (20 mg in 5 ml 100% ethanol; Sigma Chemical Co.) dissolved in 12 ml of PBS. The abdominal cavity was opened and the blood sample was obtained from aorta in heparinized tubes for further centrifugation and plasma-obtaining or EDTA-containing tubes (Hémo Kit 200; Melet Schoesing Laboratories) for blood cell counting. The intestine was then isolated and its length measured. Schematically, the intestine was divided in three identical parts in length corresponding to the duodenum, jejunum, and ileum. The proximal large intestine was isolated near the caecum and the distal part close to the rectum. The intestinal tube was washed with PBS containing 1 mM $CaCl_2$, 1 mM $MgCl_2$. Kidney was sampled and frozen in liquid nitrogen.

### Brush Border Preparations

Brush border membranes were prepared from mucosa freshly scraped from the whole small intestine. The mucosa was diluted in 10 vol/mg wt with buffer A (10 mM imidazole, 5 mM EDTA, 1 mM EGTA, pH 7.4, 0.2 mM DTT, 200 μg/ml Pefabloc, 1 μl/ml of a mixture of protease inhibitors: 1 μg/ml antipapaine, 1 μg/ml pepstatine, 15 μg/ml benzamidine) (Sigma Chemical Co.) and stirred at 4°C for 1 h. A mechanical cellular disruption was then obtained with 5 strokes in a Dounce homogeneizer (model S852; Braun). After centrifugation (10 min, 4°C, 1,000 *g*), the pellet was washed 3 times with 10 ml buffer A followed by centrifugation. At this step, two procedures were carried out: either the crude membranes were directly used for studying the $Ca^{2+}$ effect (see below) or brush border membranes were purified in a sucrose gradient. For the latter procedure, the pellet was resuspended in 10 ml buffer B (75 mM KCl, 5 mM $MgCl_2$, 1 mM EGTA, 10 mM imidazole, pH 7.4, and similar protease inhibitors to those in buffer A) and then mixed with a sucrose solution (40% sucrose final concentration in buffer B). This sample was collected in a tube containing the same volume of 65% sucrose (in buffer B), and centrifugation was performed at 4°C, 30 min, 15,000 *g*. The purified brush border membranes were obtained at the interface of the 40%:65% sucrose gradient. The protein content was determined and normalized with the initial weight of scraped mucosa.

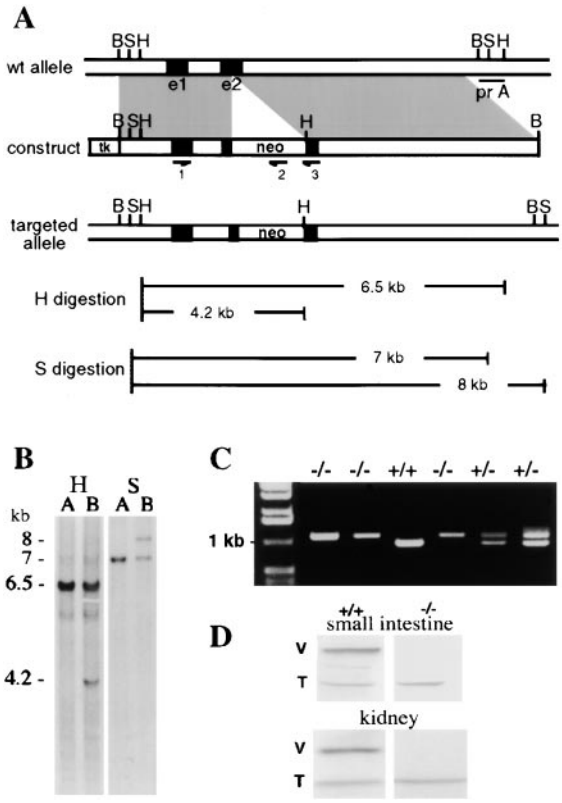


*Figure 1.* Targeted disruption of the *villin* gene. (A) Schematic representation of the expected gene replacement at the *villin* locus. Exons are represented as closed boxes (e1, e2). The neomycin resistance cassette and thymidine kinase cassette are designated neo and tk, respectively. The probe used for screening ES cell clones and genotyping mice is shown (pr A). Restriction endonuclease sites are abbreviated as follows: B, BamHI; H, HincII; S, ScaI. The PCR primers 1–3 used for genotyping are shown. wt, wild-type. (B) Southern blot analysis after HincII (H) or ScaI (S) digestions of wild-type CK35 ES cells (A) and the targeted ES cell clone (B). (C) PCR blot analysis of villin intercross progeny indicating the genotypes. The sizes were 0.9 and 1.2 kb for wild-type and homozygous bands, respectively. (D) Western blot analysis of small intestine and kidney from wild-type and villin-null mutant. No villin protein (V) was detected in the homozygous mice; tubulin (T) was used as control for quality of the protein extract.

In some experiments, brush border crude preparation was incubated for 10 min in a solution containing $10^{-5}$ to $10^{-3}$ M $CaCl_2$ in imidazole buffer (10 mM, pH 7.4, without EGTA and EDTA, plus protease inhibitors similar to those in buffer A). Microscopic observation was immediately performed using Nomarski optics (DMRD) or transmission electron microscopy after fixation (see below).

## *DNA Analysis*

DNA from embryonic stem (ES) cell pellets or mouse tails was extracted in a lysis buffer (50 mM Tris, pH 7.5, 0.1 M NaCl, 0.5% SDS, 5 mM EDTA, 100 μg/ml proteinase K), and analyzed by Southern blots or PCR.

Southern blots were performed using DNA digested with HincII or Sca1 restriction enzymes and analyzed with a 0.4 kb BamHI-HincII fragment (pr A, Fig. 1 A), and a 0.5-kb BglII-StuI fragment (data not shown) as 3′ and 5′ external probes, respectively.

PCR analysis was performed using DNA in 50 μl for 30 cycles. Each cycle consisted of 60 s at 94°C, 60 s at 67°C, and 90 s at 72°C, using the 0.5 μl of *Taq* polymerase (Quantum Biotechnologies, Inc.) in a homemade buffer (67 mM Tris HCl, pH 8.8, 16.6 mM $[NH_4]_2SO_4$, 0.45% Triton X-100, 0.2 mg/ml gelatin, 2 mM $MgCl_2$). 2 pmol of 5′-GTCAAAGGCTCTCTCAACATCAC-3′ villin sense oligonucleotide (primer 1), 1 pmol of 5′-GACTACATAGCAGTCACCATC-3′ villin antisense oligonucleotide (primer 3), and 1 pmol of 5′-TCTGGATTCATCGACTGTGGC-3′ neo antisense oligonucleotide (primer 2) were used, generating a 0.9-kb fragment for the wild-type allele and a 1.2-kb fragment for the targeted allele (Fig. 1, A and C).

## *RNA Analysis*

Total RNA was extracted from different tissues using RNA Now kit (Ozyme).

For Northern blot analysis, RNA samples (10 μg) were separated on 4.2% formaldehyde-agarose gel and blotted onto nylon membrane (Amersham). The $^{32}$P-labeled probe was synthesized with TransProbe T kit (Pharmacia Biotech). The RNA probe used corresponded to 530 bp of the 3′ end of the smaller human villin mRNA (Pringault et al., 1986).

For reverse transcription PCR analysis, 10 pmol of 5′-TCCAGCCAGCACATTCCTCTTCCC-3′ was hybridized with 2 μg of total RNA at 70°C for 10 min in distilled water. Reverse transcription with 200 U of Moloney murine leukemia virus reverse transcriptase (SuperScript II; Life Technologies, Inc.) was carried out at 37°C for 60 min in a 20 μl solution of 1× First Strand Buffer (Life Technologies, Inc.), 10 mM DTT, 0.5 mM deoxynucleoside triphosphates, and 0.4 U/ml RNasin. 3.5 μl of the resulting cDNA was amplified by PCR reaction in 50 μl for 35 cycles. Each cycle consisted of 60 s at 94°C, 60 s at 55°C, and 60 s at 72°C. 10 pmol of primers, 5′-ATGCCCAAGTCAAAGGCTCTCTCAACATCAC-3′ coding strand and 5′-TGCAACAGTCGCTGGACATCACAGG-3′ noncoding strand, was used, generating a 400-bp product.

## *Western Blot Analysis*

Proteins were separated by standard gel electrophoresis and then transferred to nitrocellulose membrane (0.2 μm; Schleicher and Schuell). Immunostaining was performed using primary antibodies visualized by peroxidase-conjugated antiimmunoglobulin antibodies (Jackson ImmunoResearch Laboratories, Inc.) or by alkaline phosphatase–conjugated antiimmunoglobulin antibodies (Promega). Quantification analysis (Vilbert Lourmat) was performed by scanning the membrane comparing the signal obtained with that obtained with anti-tubulin antibody (Amersham) for tissue and scraped mucosa or with anti–β-actin antibody (Sigma Chemical Co.) for brush border preparation.

## *Histological Analysis*

To perform histological analysis, organs from wild-type and mutant mice were dissected, fixed in formalin (10% vol/vol in PBS), ethanol dehydrated, and paraffin embedded. Sections of 5-μm width were prepared and stained with hematoxylin eosin–safranin according to standard histological procedures.

## *Immunofluorescence Microscopy*

Immunofluorescence studies were performed in cryostat sections of OCT-embedded tissues or in paraffin-embedded sections for fimbrin isoform immunodetection. 5-μm sections were prepared and fixed in 3% paraformaldehyde. After washing in PBS, permeabilization was obtained with 0.2% Triton X-100. Sections were incubated for 40 min with primary antibodies and 2% BSA, and after washing for 30 min with secondary fluorescent antibody. Control sections were obtained in the absence of primary antibody. The different antibodies that have been tested are as follows: villin (rabbit polyclonals, 1–189 affinity purified, which recognizes mainly the head piece domain [Maunoury et al., 1992], and 1–149, which recognizes both the head piece and the core region, dilution 1:50 [our unpublished data]), actin (phalloidine, dilution 1:3,000; Sigma Chemical Co.), ezrin (rabbit polyclonal, dilution 1:100; Algrain et al., 1993), fimbrin (specific antibodies against the three isoforms of fimbrin, I- T- and L-fimbrin, have been produced in rabbit and then purified by affinity; our unpublished data), brush border myosin I (BBMI) (rabbit polyclonal, dilution 1:10; kindly provided by P.T. Matsudaira, Massachusetts Institute of Technology, Cambridge, MA), espin (rabbit polyclonal, affinity purified, dilution 1:200; kindly provided by J.R. Bartles, Northwestern University Medical School, Chicago, IL), E-cadherin (DECMA, rat monoclonal, dilution 1:100; Sigma Chemical Co.), sucrase isomaltase (goat polyclonal, dilution 1:50; Riby and Kretchmer, 1984), dipeptidylpeptidase IV (CD26, rat monoclonal, dilution 1:4; Naquet et al., 1988), neutral aminopeptidase (CD13, rat ascite, dilution 1:300; kindly provided by P. Auberger, Contrat

Jeune Formation, Nice, France), alkaline phosphatase (rabbit polyclonal, affinity purified, dilution 1:500; our unpublished data), carcinoembryonic antigen (mouse monoclonal, not diluted; kindly provided by J.-L. Teillaud, Institute Curie).

## Electron Microscopy

*Transmission Electron Microscopy Studies.* Small pieces of tissue (~1–2 mm) were fixed for 2 h at room temperature in 2.5% glutaraldehyde and 2% paraformaldehyde in 80 mM cacodylate buffer, pH 7.2, 0.05% $CaCl_2$. After washing with the same buffer, the tissue was postfixed for 30 min at 4°C with 1% osmium and 1.5% potassium ferrocyanure in 80 mM cacodylate buffer, pH 7.2, and then at room temperature for 1 h with 2% uranyl acetate in 40% ethanol. The samples were dehydrated in a series of graded ethanol solutions and then embedded in Epon.

For brush border preparations, the procedure has been described previously (Burgess and Prum, 1982). In brief, the brush border membranes were fixed for 30 min at room temperature in 0.1 M phosphate buffer, pH 7.0, with 3% glutaraldehyde and 0.2% tannic acid. Washing was performed for 10 min at room temperature with 0.1 M phosphate buffer, pH 7.0, containing 10% sucrose. Postfixation was done for 1 h at 4°C in 1% osmium in 0.1 M phosphate buffer, pH 6.0. The samples were then washed three times in water and processed as above. Silver sections were contrasted and then observed with CM120 Twin microscope (Philips).

Semithin sections (0.2 μm) were stained with toluidine blue and were examined with a Leitz (DMRD) microscope.

*Fourier Analysis of the Microvilli Transverse Sections.* Images showing transverse sections through the microvilli and having a magnification of 22,000 were selected. Negatives were scanned on an Arcus II scanner (Agfa) to give a pixel size of 1.3 nm on the digitized image. All images were divided into boxes of 1,024 × 1,024 pixels to be processed using NIH image 1.60 (44 boxes for 8 wild-type animals, and 83 boxes for 12 villin-null mice). The Fourier transform and the power spectrum of each square area were calculated. Fourier analysis has allowed us to classify the specimens in three major categories (nonordered, slightly ordered, and well-ordered specimens) according to the characteristics of the power spectra of the transverse sections.

*Scanning Electron Microscopy Studies.* About 1 cm of intestine was fixed as described above for transmission electron microscopy. The intestine was then opened and fixed, luminal side up, on pieces of cork. Dehydration was then performed in a series of graded ethanol solution. The samples were dried by the critical point method using liquid $CO_2$ and coated with gold palladium. Observation was performed with a scanning electron microscope (Jeol JSM 840A).

## In Vivo Experiments

Three series of experiments were conducted.

*Pharmacological Experiments.* After mouse anesthesia, a jejunum loop was in situ isolated, taking care not to injure the local vasculature. Drugs were applied either from the apex or from the basolateral side of the intestine.

For the apical application of drugs, the intestinal loop was washed with PBS without $Ca^{2+}$ and $Mg^{2+}$. Then, ~700 μl of a solution of ionophore A23187 (10 μM [Sigma Chemical Co.] diluted in PBS) was injected in the lumen of the intestine (~3 cm) between two clamps, for 10 min. After washing with PBS, this loop was separated in two parts with a surgical clamp, and only the lower part was injected with ~300 μl of PBS containing $2 \times 10^{-4}$ M $CaCl_2$ for 30 min. This experiment was repeated in five wild-type and five villin-null mice. In separate animals, thapsigargin (1 mM; Sigma Chemical Co.) or ATP (1 mM; Sigma Chemical Co.) was injected in an isolated segment of the jejunal loop for 30 min. For each animal, a segment infused with only PBS served as control.

For the basolateral infusion of drugs, the isolated loop was carefully placed in a Petri dish containing 1 or 10 μM carbachol (Sigma Chemical Co.) in PBS plus $Ca^{2+}$ for 20 min. This experiment was repeated in two wild-type and two villin-null mice.

At the end of the experiment, the animal was killed with a lethal dose of anesthetic. The intestinal loop treated with the drug or PBS was cut and prepared as described above for transmission electron microscopy and immunofluorescence study.

*Physiological Experiments.* Experiments were performed in six awake animals (three wild-type and three mutants) after 24 h fasting with normal drinking. Then, a 60-min refeeding period was observed. The mice were then killed and the intestine was removed as described above for immunohistochemistry analysis.

*Pathological Experiments.* DSS (2.5%, wt/vol, mol wt 40,000; ICN Biomedical) was administered in the drinking water of 27 wild-type mice and 26 mutant mice for 13 consecutive days (total numbers for 5 independent experiments performed in parallel, with ~ 5 wild-type and 5 mutant mice in each series). This procedure is known to induce colic epithelial injury (Okayasu et al., 1990; Mashimo et al., 1996). Survival of the animals was surveyed during a period of 13 d. The remaining living animals were killed at day 13, and the small and large intestines were sampled as described above for histological analysis. The survival curves were analyzed by Kaplan Meier transform of probability versus days of DSS treatment. A $P$ value $<0.05$ is considered as significant.

# Results

## Generation of Villin-null Mice

1 of 150 G418-gancyclovir–resistant ES cell clones underwent homologous recombination at the *villin* locus as determined by Southern blot analysis (Fig. 1 B). Hybridization with a neo probe failed to detect any additional sites of integration (data not shown). The targeted clone was injected into host C57Bl6 blastocysts, and the blastocysts were transferred to the uteri of pseudopregnant females. Germline transmission of the mutant allele was achieved with the targeted ES clone. The heterozygous mice did not display any obvious abnormalities in comparison with their wild-type littermates.

## Villin-null Mice Are Viable and Fertile

To examine whether animals homozygous for the *villin* mutation were viable, heterozygous animals were intercrossed and genotypes of the progeny were determined by Southern blot or by PCR analysis. Mice homozygous for the villin mutation were detected among the intercross progeny (Fig. 1 C). The genotypes of the progeny showed a good fit to Mendelian distribution (+/+: 84, 27%; +/−: 148, 48%; −/−: 74, 24%). Homozygous villin-deficient mice were indistinguishable from their heterozygous or wild-type littermates on the basis of size, activity, fertility, or aging. When interbred, villin-null females had litter sizes similar to their wild-type littermates. Animals were followed for as long as 2 yr and no obvious pathology developed.

To verify the absence of villin protein in homozygous mice, we examined the small intestine, colon, and kidney. By immunofluorescence, no staining was observed in the null mutant mice contrasting with an apical brush border staining in the wild-type animals (see Fig. 4, A and B). Western blot analysis of the same tissues was performed using polyclonal antibodies which recognize either the head piece COOH-terminal domain or both this domain and the core of villin. No villin protein was detected in the mutant mice, whereas a significant amount was present in wild-type animals (Fig. 1 D). By Northern blot analysis and reverse transcription PCR, no villin mRNA was detected in the homozygous animals. No aberrant transcripts could be detected (data not shown).

Plasma values did not reveal any major differences between homozygous and wild-type animals (Na concentration: 147 mM ± 1.8, $n = 17$, and 145 mM ± 0.8, $n = 10$; glucose concentration: 14.9 mM ± 1.87, $n = 7$, and 14.3 mM ± 1.34, $n = 5$; creatinine concentration: 20.6 μM ± 3.79, $n = 5$, and 19.7 μM ± 3.14, in wild-type and villin-null mice, respectively, means ± SEM). This observation

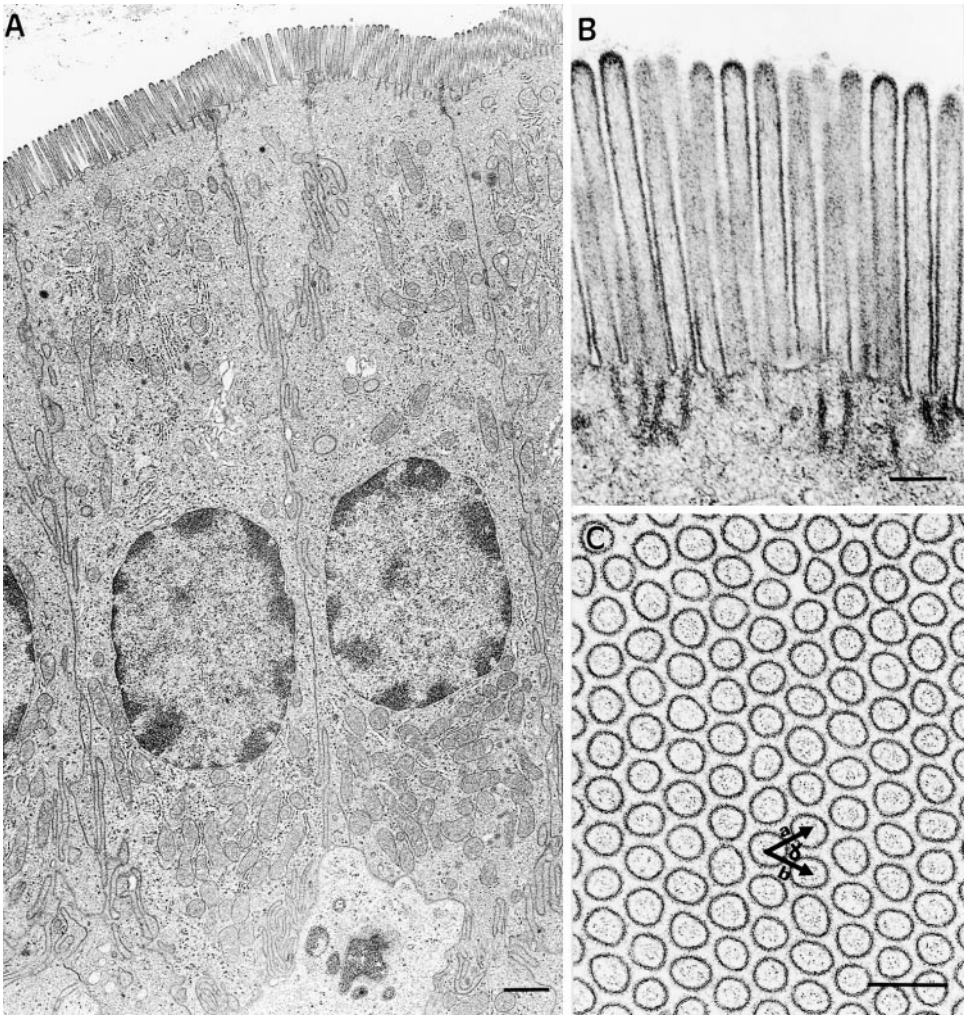


*Figure 2.* Transmission electron microscopy demonstrated morphological intact microvilli in small intestine of villin-null mice (A and B). No major difference was observed between wild-type and villin-null mice, but a large heterogeneity was always observed in the length of the microvilli. Transversal sections (C) were used for Fourier analysis, determining the ultrastructural organization of the microvilli. A and B represent the distance between two neighboring microvilli, and $\gamma$ the lattice angle between these directions. Bar, 1 $\mu$m (A) and 0.2 $\mu$m (B and C).

suggests, in a first approximation, that the transport functions of intestine and kidney were unaffected under basal conditions. This hypothesis could be indirectly correlated to the normal distribution in the intestinal epithelial cells of the major digestive enzymes. Indeed, the different enzymes—sucrase isomaltase, dipeptidylpeptidase IV, neutral aminopeptidase, and alkaline phosphatase—that have been studied by immunofluorescence have a normal localization in both wild-type and villin-null mice (data not shown).

### *Brush Border Is Unaffected in the Absence of Villin*

Careful examination of histological sections and of scanning electron microscopy pictures of the different parts of intestine, duodenum, jejunum, ileum, and proximal and distal colon did not detect any differences in histological appearance between wild-type and mutant mice (data not shown).

At the cellular level, transmission electron microscopy revealed no difference on brush border microvilli structure in homozygous mice compared with wild-type (Fig. 2). Large heterogeneity in the length of the microvilli was observed in both wild-type and mutant mice. Fourier analysis was used as a quantitative method to describe the long range organization of the microvillus array. Representatives of all the defined categories, nonordered, slightly ordered, and well-ordered specimens (see Materials and Methods), indicating intra- and interindividual variations in the organization of the microvilli, were found in both wild-type and homozygote animals with a similar median. The percentage of the well-ordered crystalline lattices was similar for homozygote (34/83, 41%) and wild-type (14/44, 32%) mice ($\chi^2$ test, $P > 0.5$). These crystalline lattices were characterized by the distance between two neighboring microvilli (a and b) and the lattice angle between these directions ($\gamma$) (see Fig. 2 C). The mean values are a = 119 $\pm$ 1.4 nm (mean $\pm$ SEM), b = 109 $\pm$ 1.8 nm, and $\gamma$ = 58 $\pm$ 1.6° in wild-type animals (14 sections, $n$ = 8), and a = 114 $\pm$ 2.1 nm, b = 107 $\pm$ 1.8 nm, and $\gamma$ = 59 $\pm$ 0.92° in mutant animals (34 sections, $n$ = 12), indicating no obvious difference ($t$ test, $P < 0.05$) in microvilli organization between these animals.

To examine whether other actin-binding proteins take over the bundling activity of villin, protein extracts from purified brush border preparation and immunofluorescence staining of intestine sections were performed. Semiquantitative Western blot analysis of the three fimbrin isoforms (I, T, and L), espin, and ezrin as well as immunofluorescence staining (fimbrin isoforms, espin, ezrin, and BBMI) did not reveal any major difference between wild-type and homozygous animals. However, a slight increase in the la-

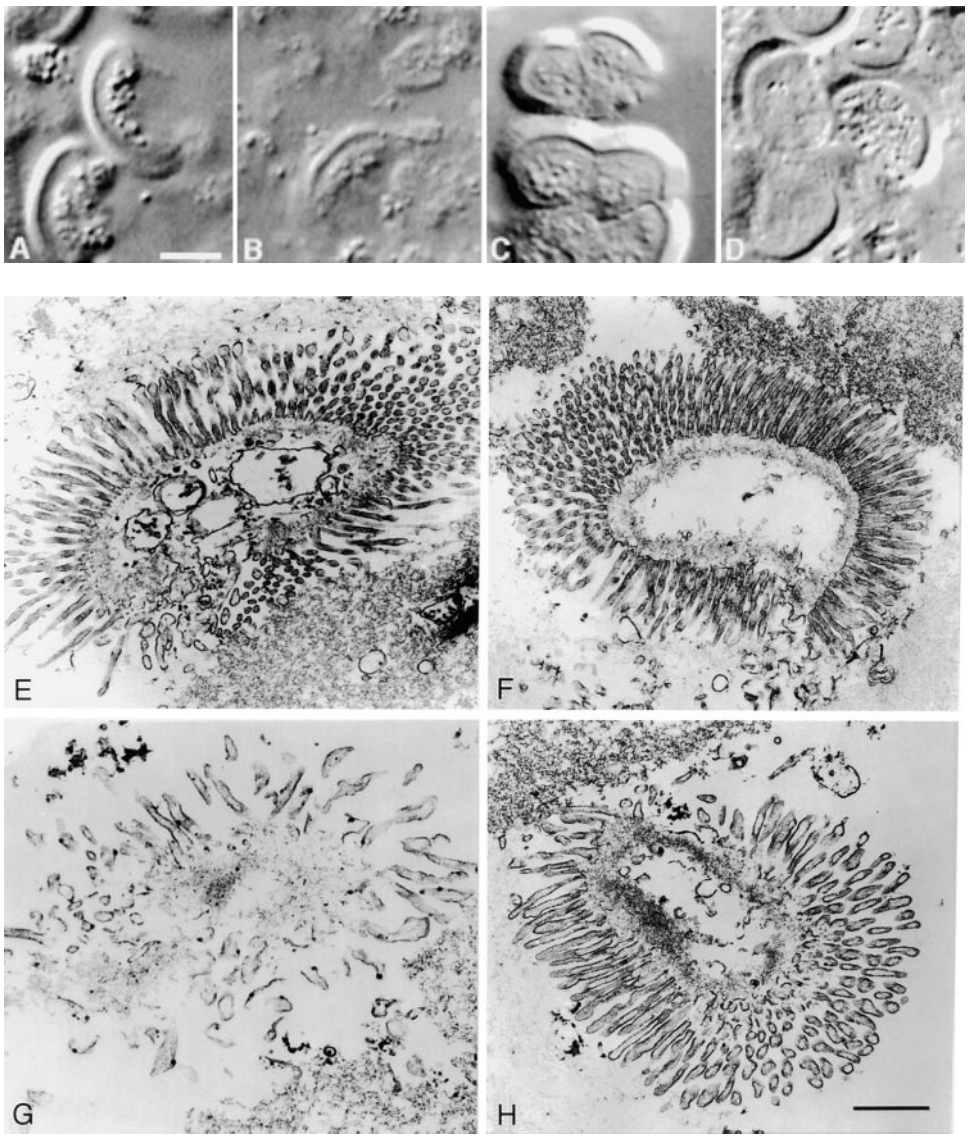


*Figure 3.* Brush border preparation from wild-type animals (A, B, E, and G) and villin-null mice (C, D, F, and H). Brush borders were observed by Nomarski (A–D) or by transmission electron microscopy (E–H). Two experimental conditions were performed: in the absence of $Ca^{2+}$ (A, C, E, and F), and in presence of $10^{-4}$ M $Ca^{2+}$ for 10 min (B, D, G, and H). It should be noticed that in wild-type animals in the presence of $Ca^{2+}$, it is very difficult to recognize the structure of the brush border, as most of them are vesiculated. Bar, 5 μm (A–D) and 1 μm (E–H).

beling intensity of espin was systematically noticed in the mutant mice. This observation could be related to a better accessibility to espin epitopes in the absence of villin. Indeed, semiquantitative analysis of Western blot performed on brush border preparation failed to demonstrate any increase in espin concentration in villin-null mice. These results indicate that these known actin-binding proteins of the brush border microvilli are neither overexpressed nor downregulated in the absence of villin.

### *$Ca^{2+}$-dependent Disruption of F-actin Is Impaired in the Absence of Villin*

To examine $Ca^{2+}$-dependent severing of actin in villin-null mice, both in vitro and in vivo approaches were undertaken. In vivo, pharmacological, physiological, and pathological conditions were explored.

In vitro, when brush borders were isolated in the absence of $Ca^{2+}$ and purified on sucrose gradient, a marked difference was observed between wild-type and mutant mice. On average, a threefold increase in the yield of brush border recovery, calculated as the ratio of final protein content over initial mucosa weight, was obtained in the villin-null mice compared with wild-type. This observation suggests that the mutant mice brush borders were less fragile to mechanical cell disruption. Both wild-type and mutant mice presented a tightly packed array of microvilli (Fig. 3, A and C) and a well-conserved ultrastructure with a normal actin filament bundle (Fig. 3, E and F). The addition of $Ca^{2+}$ in wild-type preparation (final concentration $10^{-5}$ to $10^{-3}$ M) resulted in a rapid alteration of brush borders (Fig. 3, B and G) where the microvillar core disassembled with the concomitant vesiculation of the surrounding membrane. In contrast, the morphology of mutant mouse brush border remained unchanged in the presence (Fig. 3, D and H) or absence of $Ca^{2+}$ (Fig. 3, C and F) as assessed by both optical Nomarski observation and transmission electron microscopy. These results demonstrated that, in the absence of villin, no fragmentation activity upon actin filaments occurred in response to increased $Ca^{2+}$ concentrations.

In vivo, in pharmacological experiments, jejunum loops

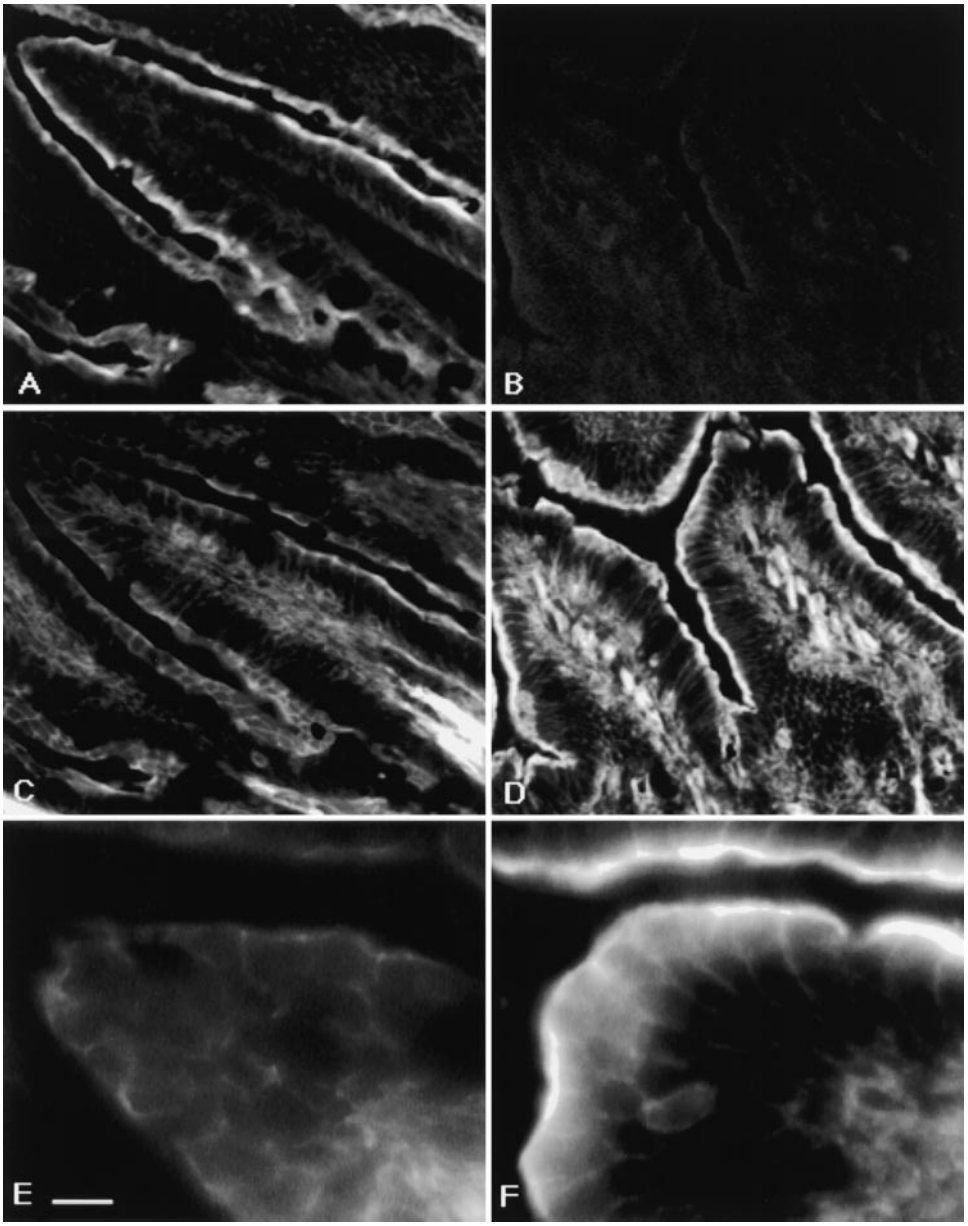


*Figure 4.* Immunofluorescence of villin (A and B) and actin (C–F) in the small intestine after the basolateral application of carbachol (10 μM) in wild-type (A, C, and E) and villin-null (B, D, and F) mice. Similar results were obtained with 1 μM carbachol (data not shown). Bar, 15 μm (A–D) and 7 μm (E and F).

isolated in situ were used to test the effect of $Ca^{2+}$. Different strategies known to increase intracellular $Ca^{2+}$ concentration were monitored using ATP, carbachol, an acetylcholine agonist, $Ca^{2+}$ ionophore A23187, or thapsigargin, a blocker of the endoplasmic reticulum $Ca^{2+}$ ATPase. In the brush border from wild-type small intestine, the major effect observed with each of these conditions was a disruption of the apical F-actin phalloidin labeling, as illustrated in Fig. 4, C and E, using 10 μM carbachol basolateral treatment in comparison to the intense and broad F-actin labeling observed in the untreated wild-type animal (see Fig. 5 A). Only thin phalloidin labeling remained at the apical pole, probably related to the terminal web region; the basolateral F-actin labeling was unaltered. Slight differences were noticed using the various conditions to increase intracellular $Ca^{2+}$ concentration: carbachol basolateral treatment affected the apical labeling all along the villus, whereas the others drugs, administered in the lumen of the intestine, altered mostly the upper part of the villus, probably due to differences in accessibility of the drug. In these animals, the villin labeling was unaffected (Fig. 4 A). In contrast, in the villin-null mice, whatever conditions were used to increase $Ca^{2+}$, the phalloidin F-actin labeling was unaffected: a large continuous F-actin ribbon (Fig. 4, D and F) was observed along the villi similar to that observed in both control wild-type and villin-null mice (Fig. 5, A and B). No significant alteration of the microvilli structure was observed by transmission electron microscopy on fixed tissues. This discrepancy between electron and light microscopy observations may be due to the different procedures and processing of the specimens (i.e., fixatives and freezing). Alternatively, rapidly reversible effects may have occurred, as it has been shown in primary culture of proximal tubule for the $Ca^{2+}$-dependent effect of parathormone (Goligorsky et al., 1986). To assess this hypothesis in our in vivo conditions, extensive kinetics

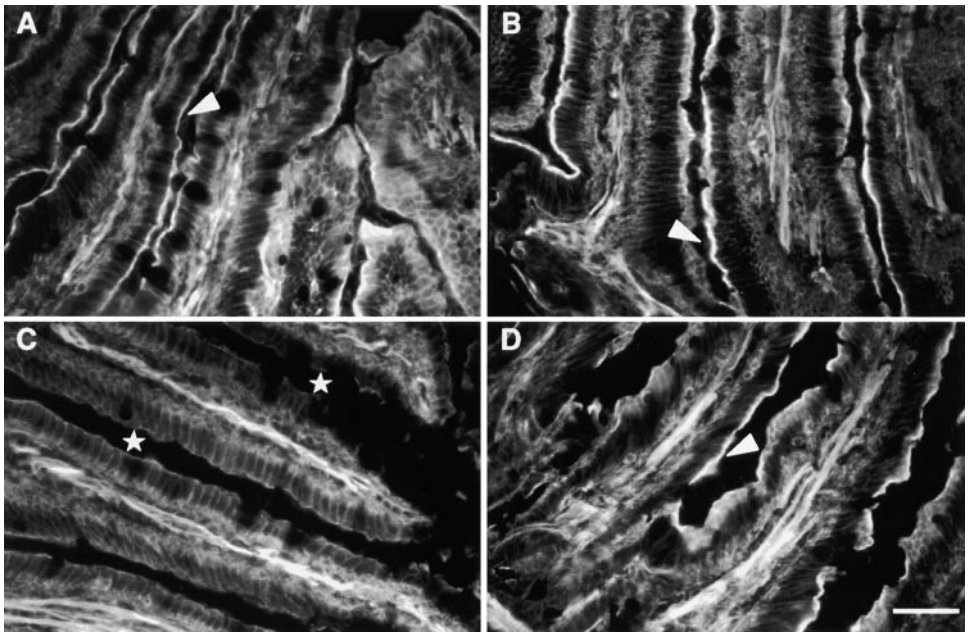


*Figure 5.* Immunofluorescence of F-actin (phalloidin labeling) in the small intestine from control animals (A and B) or after fasting/refeeding experiments (C and D) in wild-type (A and C) and villin-null mice (B and D). Arrows indicate normal F-actin labeling of the brush borders. Stars indicate a weak residual staining. Bar, 15 μm.

studies have to be performed in a large series of animals.

In vivo, in a physiological fasting/refeeding condition, most of the apical phalloidin labeling disappeared in wild-type animals, whereas in villin-null mice, it remained unaffected (Fig. 5, C and D). This alteration affected the whole length of intestinal villi similarly in the three animals.

In pathological experiments where colitis was induced by DSS administration, although some variation was observed in the series of five experiments, villin-null mice appeared to be significantly more sensitive to the injuring effect of the DSS treatment. This is illustrated by the fact that 64% of mutant animals are dead at day 13 in contrast to only 30% of wild-type animals (Kaplan Meier transform, $P = 0.008$; Fig. 6 A). The median survival time was 10 d for the mutant mice; this parameter cannot be defined for the wild-type animals. Multiple and extended sites of epithelial injury were conspicuously found in the villin-null colons compared with wild-type animals (Fig. 6 B). These lesions included obvious large ulcerations, glandular atrophy, and inflammatory changes including neutrophil infiltrate, edema, and fibrosis (Fig. 6 B, panels b and d). In contrast, the wild-type colon lesions were less severe and limited to focal regions (Fig. 6 B, panels a and c). No alteration was observed along the small intestine.

## *Discussion*

Villin is one of the major structural actin-binding proteins associated with the actin cytoskeleton of the intestinal epithelial cell brush border microvilli. Among the actin-binding protein family, villin is the only member which has severing, capping, nucleating, and bundling in vitro activities. In vivo, the search for these properties needs to be performed at the level of the tissue, organ, or organism. In this study, we have addressed the biological role of villin by generating mutant mice lacking villin through homologous recombination in ES cells. In the villin-null mice, the ultrastructure of the intestinal brush border is not modified, suggesting normal bundling of the actin filaments. The other proteins expressed in the brush border (fimbrin, espin, BBM1, ezrin) are not overexpressed to compensate for the absence of villin. Interestingly, however, the severing properties of villin are not compensated in vivo, as demonstrated by the absence of actin fragmentation when the intracellular $Ca^{2+}$ concentration was increased in mutant animals.

Villin contains at least three actin-binding sites, two of which are $Ca^{2+}$ dependent and located in the core domain. The third is situated in the head piece domain and is $Ca^{2+}$ independent. The in vitro activities of villin upon actin vary with the $Ca^{2+}$ concentration (Fig. 7). At high $Ca^{2+}$ concentration ($>10^{-4}$ M), villin severs F-actin into short filaments. At lower concentration ($10^{-7}$ to $10^{-6}$ M), villin caps the fast-growing end of actin microfilament and thereby prevents elongation. At the same $Ca^{2+}$ concentration, villin nucleates microfilament growth when added to actin monomers. At very low $Ca^{2+}$ concentration ($<10^{-7}$ M), villin has no effect on actin polymerization but bundles actin filaments. In fibroblast cell culture, synthesis of large amounts of villin in cells which do not normally produce this protein induces both the growth of microvilli on the cell surface and the redistribution of F-actin. Villin lacking one actin-binding domain located at its COOH-terminal end did not induce growth of microvilli or stress fiber disruption (Friederich et al., 1989). Moreover, it has been demonstrated that a cluster of charged amino acid residues (KKEK) is crucial for the morphological activity of villin, indicating that this motif is part of an F-actin binding site that induces G-actin to polymerize (Friederich et al., 1992). Similar bundling properties of villin were demonstrated with a different approach using an antisense mRNA strategy in a colonic adenocarcinoma cell line. Indeed, stable expression of a cDNA encoding antisense villin RNA and thus downregulation of endogenous villin messenger induced dramatic brush border disassembly (Costa de Beauregard et al., 1995). The key role of villin in

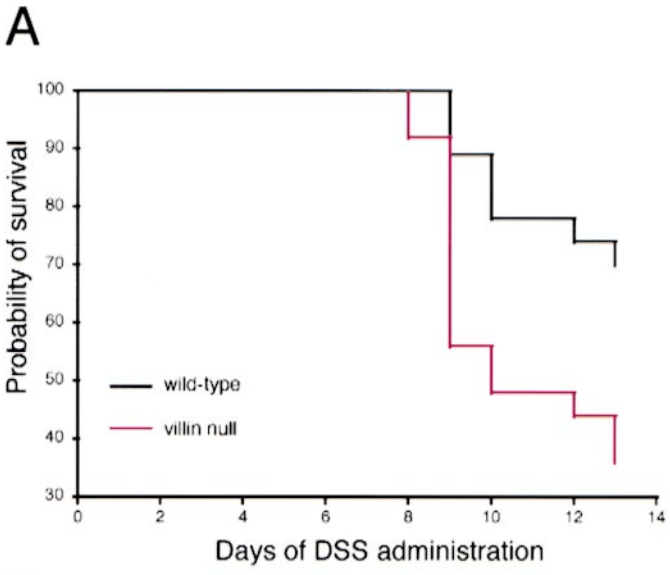


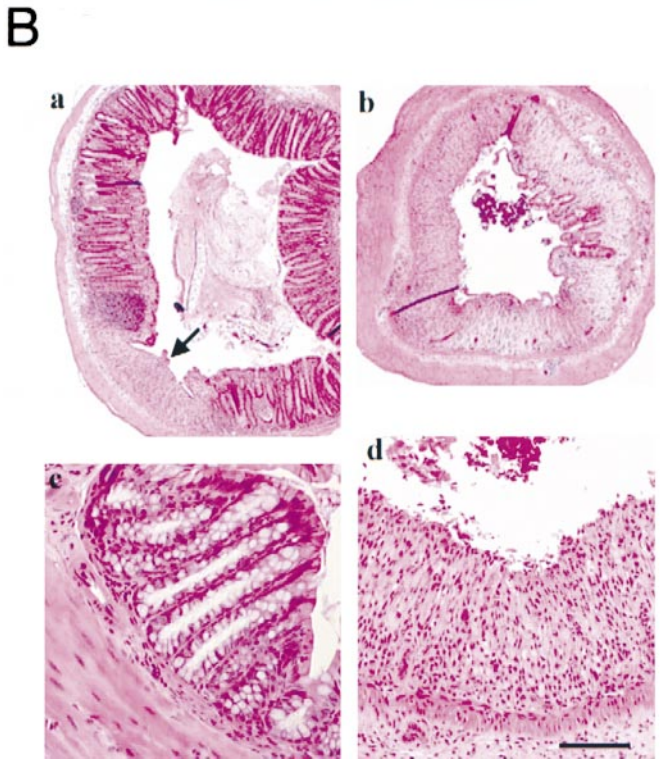


*Figure 6.* Increased DSS-induced death due to severe colonic injuries in villin-null mice. (A) Survival is diminished in villin-null mice, shown as Kaplan-Meier transform of probability versus days of DSS treatment. The survival percentages after 8, 10, and 13 d of DSS treatment were 100, 78 ± 8.0, and 70 ± 8.8% in wild type animals ($n$ = 27) versus 92 ± 5.4, 48 ± 10.0, and 36 ± 9.6% in villin-null mice ($n$ = 26) (means ± SEM). Black line, wild-type animals. Red line, villin-null mice. (B) Histological examination of proximal colon from DSS-treated wild-type (panels a and c) and villin-null mice (panels b and d). Representative areas of the lesions observed are shown in panel c (limited submucosal infiltration by inflammatory cells in wild-type colon) and d (massive loss of epithelial cells, surface and crypts, observed in extended regions in villin-null mice). A similar but focal lesion in the wild-type colon is indicated by an arrow in panel a. Bar, 1 mm (panels a and b) and 200 μm (panels c and d).

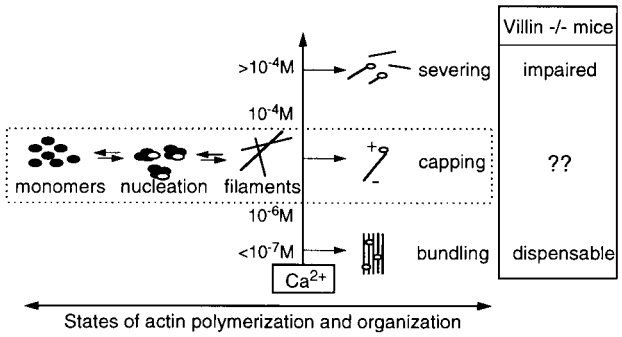


*Figure 7.* In vivo consequences of the lack of villin expression considering the different states of actin polymerization and organization as a function of $Ca^{2+}$ concentration. Filled circles, actin monomers; open circles, villin; black line, actin filament.

the morphogenesis of microvilli has not been verified in vivo (Pinson et al., 1998; this study). Indeed, both the length and the structural organization of the microvilli, in the null mouse intestine and colon are indistinguishable from those in wild-type animals. Even a sophisticated mathematical analysis of the microvilli organization such as Fourier analysis fails to demonstrate any significant difference. However, the heterogeneity observed in both types of animals may have prevented us from detecting significant differences. Nevertheless, because of the large number of animals studied in this paper and in one published previously (Pinson et al., 1998), we believe that had they existed, structural alterations should have been detected. The discrepancy between the in vivo studies and cell culture experiments is presumably due to the adaptation and plasticity of gene expression during organogenesis in vivo, properties that are lost or inefficient in in vitro systems.

Other actin-binding proteins are expressed in the brush border of epithelial cells (I isoform of fimbrin, BBMI, ezrin, and espin). Fimbrin is required, with villin, to bundle actin filaments in vitro (Coluccio and Bretscher, 1989). Three fimbrin isoforms have been demonstrated with relatively specific cell expression: I in intestine and kidney epithelial cells, L in hemopoietic cells and many tumor cell lines, and T in various cells and tissues (Chafel et al., 1995). In villin-null mice, I fimbrin exhibited a cellular distribution and a semiquantitative expression similar to those observed in wild-type animals. No expression or labeling of the T and L isoforms was observed in the brush border. In addition, no modification was noticed for espin, another actin-binding protein localized in the intestinal epithelial cells (Bartles et al., 1996, 1998) for which an actin bundling function has been demonstrated. The expression and distribution of the other actin-binding proteins present in the brush border (ezrin and BBMI) were also not modified. They do not bundle actin filaments but are involved in the link between the brush border cytoskeleton and the plasma membrane. Ezrin is known to play a structural and regulatory role in the assembly and stabilization of specialized plasma membrane domains (Bretscher et al., 1997). BBMI has been reported to connect laterally the microfilament core with the microvillus membrane (Matsudaira and Burgess, 1979). The different

members of the gelsolin/villin family of actin regulatory protein, if they are able to bundle actin in vivo as suggested by the presence of homologous COOH-terminal head piece sequences, would be good candidates to compensate for the absence of villin and might explain the normal organization of actin microfilament bundles in villin-null mice.

The $Ca^{2+}$-regulated severing properties of villin have been established mainly in vitro. This study is the first report, to our knowledge, that supports a role for the villin-severing activity in vivo. In a normal situation, at the usual low intracellular $Ca^{2+}$ concentration, the severing properties of villin should not be effective. However, a local increase of $Ca^{2+}$ can occur in some physiological conditions, such as hormonal stimulation. In these conditions, in the cells expressing villin, severing of F-actin microfilaments would be induced, a phenomenon that can be part of the hormonal response. To test the role of villin in physiological or pathological situations, we have used different pharmacological (e.g., A23187, carbachol) or physiological (fasting/refeeding) strategies, to increase the intracellular $Ca^{2+}$ concentration. For each of them, a net decrease of the F-actin microfilament labeling with phalloidin was observed only in wild-type animals, a result that suggests a severing effect of villin. In fasting/refeeding experiments, $Ca^{2+}$ concentration should also increase. Indeed, in these conditions, catecholamine and digestive hormones increases are expected, and subsequently induce an increase in the intracellular $Ca^{2+}$ concentration. Other reports also support this hypothesis. In the ileum, it has been demonstrated that F-actin fragmentation is necessary for carbachol to inhibit NaCl absorption (Khurana et al., 1997). The cholinergic agonist carbachol activates basolateral M3 muscarinic cholinergic receptors and then induces a biphasic increase in intracellular $Ca^{2+}$ concentration involving a phosphoinositol phospholipase/phosphokinase (PLC/PKC) cascade (for review see Donowitz et al., 1998). The physiological effect of carbachol consists of an inhibition of the NaCl absorption and brush border $Na^+/H^+$ exchange (Cohen et al., 1991), presumably as a result of the internalization of the transport proteins (Donowitz, M., personal communication).

Another situation in which modifications of intracellular $Ca^{2+}$ concentration occurs is during infection by microorganisms or during different conditions that induce cell injury (e.g., acid application, stress, wounding). During the intestinal infections by enteroaggregative or enteropathogenic *Escherichia coli* (EAEC, EPEC), vesiculation of the brush border has been observed (for review see Garcia and Le Bouguénec, 1996). The increased $Ca^{2+}$ concentration induced by the bacterial infection might rearrange the cytoskeleton and activate $Ca^{2+}$-dependent kinase(s) resulting in morphological changes such as microvilli effacement and pedestal formation in the host cells. Damage of the intestinal mucosa has also been investigated by the use of DSS, a chemical agent that induces acute and chronic experimental ulcerative colitis in mice (Okayasu et al., 1990). DSS also causes changes in the intestinal microflora. This alteration, which can be compared with pathological intestinal infection, together with inappropriate macrophage function or toxic effects on colonic epithelium, is a possible mechanism by which enteral DSS induces ulcerative colitis in experimental animals. The observation that the death probability was two times higher in villin-null mice compared with wild-type suggests that villin might be involved in the cell injury processes and/or in the cell repairing processes. The exact role of villin in these processes remains to be further investigated. A working hypothesis is that the binding of villin to F-actin microfilaments plays a key role in the dynamics of the actin cytoskeleton, and therefore it might be a major factor in cell organization and motility. Interestingly, the present result may also have clinical implications. Indeed, the etiology of the human hemorrhagenic colorectitis is still unknown. Considering the large extension of the colon lesions in villin-null mice after DSS, an alteration of villin, such as a *villin* gene mutation, could be an interesting etiologic hypothesis for this pathology.

This study illustrates the complexity of the protein interactions at the cellular, tissue, organ, and animal levels. During mouse development, mechanisms might be used to compensate for the absence of villin and thus to organize well-structured microvilli in intestinal cells. In the adult mouse, this compensation persists and results in an apparently normal intestinal epithelium. We can postulate that fimbrin may play a role to compensate for the bundling activity of villin that leads to obtain normal morphogenesis, whereas no other actin-binding protein could efficiently provide the severing activity necessary for the dynamics of cortical actin microfilaments in enterocytes. This proposal can be evaluated in future experiments by creating villin- and fimbrin-null mice.

Moreover, cellular apoptosis that occurred at the upper part of the villi was similar in villin-null mice and in the wild-type animals (data not shown). Thus, the equilibrium between living and apoptotic cells in the intestine is maintained under physiological conditions in the mutant mice. As illustrated in this work, after inducing cell injury by the administration of DSS, the lack of epithelial cell plasticity might lead to dramatic effects. Starvation, unbalanced diet, cell injury, local infections, and carcinogenesis are stresses that might affect the dynamics of brush border F-actin microfilaments. Indeed, it is well established that actin microfilaments are essential to remodel cell shape and to drive cell motility. Hence, external stimuli leading, for instance, to epithelial plasticity and cell repair could be required in a variety of conditions in which villin-null mice might be found deficient in the course of future investigations.

We are grateful to Monique Arpin for her skillful advice in preparing fimbrin isoform antibodies, Julio Celis for his help in protein analysis, Hubert Reggio for his study of the Peyer's patches, Fabiola Terzi for performing transient renal ischemia, Daniel Meur and Dominique Morineau for the transmission electron microscopy photographic artwork, and Emmanuelle Fourme from the Biostatistics Department of Curie Hospital (Prof. Bernard Asselain) and Frédéric Fumeron (Laboratoire de Nutrition, Faculté Xavier Bichat) for the statistical analysis of the survival of the mice after DSS treatment. We also thank Manuel Buchwald, Evelyne Coudrier, Evelyne Friederich, and Thierry Galli for their helpful comments and valuable discussions. The scanning microscopy was performed at Centre Interuniversitaire de Microscopie Electronique (CIME) with the technical assistance of Michèle Grasset.

This work was supported in part by Association de Recherche contre le Cancer, Ligue Nationale contre le Cancer, Centre National de la Recherche Scientifique, Institut Pasteur, and Institut Curie. A. Lapillonne was a recipient of an Ipsen Laboratories fellowship.

Submitted: 25 November 1998
Revised: 24 May 1999
Accepted: 25 June 1999

*References*

Algrain, M., O. Turunen, A. Vaheri, D. Louvard, and M. Arpin. 1993. Ezrin contains cytoskeleton and membrane binding domains accounting for its proposed role as a membrane-cytoskeletal linker. *J. Cell Biol.* 120:129–139.

Ampe, C., and J. Vandekerckhove. 1987. The F-actin capping proteins of *Physarum polycephalum*: cap42(a) is very similar, if not identical, to fragmin and is structurally and functionally very homologous to gelsolin; cap42(b) is *Physarum* actin. *EMBO (Eur. Mol. Biol. Organ.) J.* 6:4149–4157.

André, E., F. Lottspeich, M. Schleicher, and A. Noegel. 1988. Severin, gelsolin, and villin share a homologous sequence in regions presumed to contain F-actin severing domains. *J. Biol. Chem.* 263:722–727.

Arpin, M., E. Pringault, J. Finidori, A. Garcia, J.-M. Jeltsch, J. Vandekerckhove, and D. Louvard. 1988. Sequence of human villin: a large duplicated domain homologous with other actin-severing proteins and a unique small carboxy-terminal domain related to villin specificity. *J. Cell Biol.* 107:1759–1766.

Bader, M.F., J.M. Trifaro, O.K. Langley, D. Thierse, and D. Aunis. 1986. Secretory cell actin-binding proteins: identification of a gelsolin-like protein in chromaffin cells. *J. Cell Biol.* 102:636–646.

Bartles, J.R., A. Wierda, and L. Zheng. 1996. Identification and characterization of espin, an actin-binding protein localized to the F-actin–rich junctional plaques of *Sertoli* cell ectoplasmic specializations. *J. Cell Sci.* 109:1229–1239.

Bartles, J.R., L. Zheng, A. Li, A. Wierda, and B. Chen. 1998. Small espin: a third actin-bundling protein and potential forked protein ortholog in brush border microvilli. *J. Cell Biol.* 143:107–119.

Bazari, W.L., P.T. Matsudaira, M. Wallek, J. Smeal, R. Jakes, and Y. Ahmed. 1988. Villin sequence and peptide map identify six homologous domains. *Proc. Natl. Acad. Sci. USA.* 85:4986–4990.

Bradley, A. 1987. Production and analysis of chimaeric mice. *In* Teratocarcinomas and Embryonic Stem Cells: A Practical Approach. E.J. Robertson, editor. IRL Press, Oxford.

Bretscher, A., and K. Weber. 1979. Villin: the major microfilament-associated protein of the intestinal microvillus. *Proc. Natl. Acad. Sci. USA.* 76:2321–2325.

Bretscher, A., and K. Weber. 1980. Villin is a major protein of the microvillus cytoskeleton which binds both G and F actin in a calcium-dependent manner. *Cell.* 20:839–847.

Bretscher, A., D. Reczek, and M. Berryman. 1997. Ezrin: a protein requiring conformational activation to link microfilaments to the plasma membrane in the assembly of cell surface structures. *J. Cell Sci.* 110:3011–3018.

Burgess, D.R., and B.E. Prum. 1982. Reevaluation of brush border motility: calcium induces core filament solation and microvillar vesiculation. *J. Cell Biol.* 94:97–107.

Chafel, M.M., W. Shen, and P. Matsudaira. 1995. Sequential expression and differential localization of I-, L-, and T-fimbrin during differentiation of the mouse intestine and yolk sac. *Dev. Dyn.* 203:141–151.

Cohen, M.E., J. Wesolek, J. McCullen, K. Rys-Sikora, S. Pandol, R.P. Rood, G.W.G. Sharp, and M. Donowitz. 1991. Carbachol- and elevated $Ca^{2+}$-induced translocation of functionally active protein kinase C to the brush border of rabbit ileal $Na^+$ absorbing cells. *J. Clin. Invest.* 88:855–863.

Cohen-Tannoudji, M., S. Robine, A. Choulika, D. Pinto, F. El Marjou, C. Babinet, D. Louvard, and F. Jaisser. 1998. I-*Sce*I-induced gene replacement at a natural locus in embryonic stem cells. *Mol. Cell. Biol.* 18:1444–1448.

Coluccio, L.M., and A. Bretscher. 1989. Reassociation of microvillar core proteins: making a microvillar core in vitro. *J. Cell Biol.* 108:495–502.

Costa de Beauregard, M.A., E. Pringault, S. Robine, and D. Louvard. 1995. Suppression of villin expression by antisense RNA impairs brush border assembly in polarized epithelial intestinal cells. *EMBO (Eur. Mol. Biol. Organ.) J.* 14:409–421.

Donowitz, M., S. Khurana, C.M. Tse, and C.H.C. Yn. 1998. G protein-coupled receptors in gastrointestinal physiology. III. Asymmetry in plasma membrane signal transduction: lessons from brush border $Na^+/H^+$ exchangers. *Am. J. Physiol.* 274:G971–G977.

Friederich, E., C. Huet, M. Arpin, and D. Louvard. 1989. Villin induces microvilli growth and actin redistribution in transfected fibroblasts. *Cell.* 59: 461–475.

Friederich, E., E. Pringault, M. Arpin, and D. Louvard. 1990. From the structure to the function of villin, an actin-binding protein of the brush border. *Bioessays.* 12:403–408.

Friederich, E., K. Vancompernolle, C. Huet, M. Goethals, J. Finidori, J. Vandekerckhove, and D. Louvard. 1992. An actin-binding site containing a conserved motif of charged amino acid residues is essential for the morphogenic effect of villin. *Cell.* 70:81–92.

Garcia, M.I., and C. Le Bouguénec. 1996. Role of adhesion in pathogenicity of human uropathogenic and diarrhoeogenic *Escherichia coli*. *Bull. Inst. Pasteur.* 94:201–236.

Glenney, J.R., and P. Glenney. 1985. Comparison of $Ca^{++}$-regulated events in the intestinal brush border. *J. Cell Biol.* 100:754–763.

Glenney, J.R., A. Bretscher, and K. Weber. 1980. Calcium control of the intestinal microvillus cytoskeleton: its implications for the regulation of microfilaments organizations. *Proc. Natl. Acad. Sci. USA.* 77:6458–6462.

Glenney, J.R.J., and K. Weber. 1981. Calcium control of microfilaments: uncoupling of the F-actin-severing and -bundling property of villin by limited proteolysis in vitro. *Proc. Natl. Acad. Sci. USA.* 78:2810–2814.

Goligorsky, M.S., D.N. Menton, and K.A. Hruska. 1986. Parathyroid hormone-induced changes of the brush border topography and cytoskeleton in cultured renal proximal tubular cells. *J. Membr. Biol.* 92:151–162.

Khurana, S., M. Arpin, R. Patterson, and M. Donowitz. 1997. Ileal microvillar protein villin is tyrosine-phosphorylated and associates with PLC-$\gamma_1$. *J. Biol. Chem.* 272:30115–30121.

Knutton, S., T. Baldwin, P. Williams, A. Manjarrez-Hernandez, and A. Aitken. 1993. The attaching and effacing virulence activity of enteropathogenic *Escherichia coli*. *Int. J. Med. Microbiol. Virol. Parasitol. Infect. Dis.* 278:209–217.

Kress, C., S. Vandormael-Pournin, P. Baldacci, M. Cohen-Tannoudji, and C. Babinet. 1998. Nonpermissiveness for mouse embryonic stem (ES) cell derivation circumvented by a single backcross to 129/Sv strain: establishment of ES cell lines bearing the Omd conditional mutation. *Mamm. Genome.* 9:998–1001.

Kwiatkowski, D.J., T.P. Stossel, S.H. Orkin, J.E. Mole, H.R. Colten, and H.L. Yin. 1986. Plasma and cytoplasmic gelsolins are encoded by a single gene and contain a duplicated actin-binding domain. *Nature.* 323:455–458.

Marcu, M.G., A.R. del Castillo, M.L. Vitale, and J.M. Trifaro. 1994. Molecular cloning and functional expression of chromaffin cell scinderin indicates that it belongs to the family of $Ca^{2+}$-dependent F-actin severing proteins. *Mol. Cell. Biochem.* 141:153–165.

Marks, P.W., M. Arai, J.L. Bandura, and D.J. Kwiatkowski. 1998. Advillin (p92): a new member of the gelsolin/villin family of actin regulatory proteins. *J. Cell Sci.* 111:2129–2136.

Mashimo, H., D.-C. Wu, D.K. Podolsky, and M.C. Fishman. 1996. Impaired defense of intestinal mucosa in mice lacking intestinal trefoil factor. *Science.* 274:262–265.

Matsudaira, P.T., and D.R. Burgess. 1979. Identification and organization of the components in the isolated microvillus cytoskeleton. *J. Cell Biol.* 83:667–673.

Matsudaira, P.T., and D.R. Burgess. 1982. Partial reconstitution of the microvillus core bundle: characterization of villin as a $Ca^{2+}$-dependent, actin-bundling/depolymerization protein. *J. Cell Biol.* 92:648–656.

Maunoury, R., S. Robine, E. Pringault, N. Leonard, J.A. Gaillard, and D. Louvard. 1992. Developmental regulation of villin gene expression in the epithelial cell lineages of mouse digestive and urogenital tracts. *Development.* 115: 717–728.

Misch, S.W., P.E. Giebel, and R.G. Faust. 1980. Intestinal microvilli: responses to feeding and fasting. *Eur. J. Cell Biol.* 21:269–279.

Mooseker, M.S. 1985. Organization, chemistry, and assembly of the cytoskeletal apparatus of the intestinal brush border. *Annu. Rev. Cell Biol.* 1:209–241.

Mooseker, M.S., T.A. Graves, K.A. Wharton, N. Falco, and C.L. Howe. 1980. Regulation of microvillus structure: calcium-dependent solation and cross-linking of actin filaments in the microvilli of intestinal epithelial cells. *J. Cell Biol.* 87:809–822.

Naquet, P., H.R. Macdonald, P. Brekelmans, J. Barbet, S. Marchetto, W. Van Ewijk, and M. Pierres. 1988. A novel T cell-activated molecule (THAM) highly expressed on CD4−CD8− murine thymocytes. *J. Immunol.* 141: 4101–4109.

Northrop, J., A. Weber, M. Mooseker, C. Armstrong, M. Bishop, G. Dubyak, M. Tucker, and T. Walsh. 1986. Different calcium dependence of the capping and cutting activities of villin. *J. Biol. Chem.* 261:9274–9281.

Okayasu, I., S. Hatakeyama, M. Yamada, T. Ohkusa, Y. Inagaki, and R. Nakaya. 1990. A novel method in the induction of reliable experimental acute and chronic ulcerative colitis in mice. *Gastroenterology.* 98:694–702.

Pestonjamasp, K.N., R.K. Pope, J.D. Wulkuhle, and E.J. Luna. 1997. Supervillin (p205): a novel membrane-associated, F-actin–binding protein in the villin/gelsolin superfamily. *J. Cell Biol.* 139:1255–1269.

Pinson, K.I., L. Dunbar, L. Samuelson, and D.L. Gumucio. 1998. Targeted disruption of the mouse villin gene does not impair the morphogenesis of microvilli. *Dev. Dyn.* 200:109–121.

Pringault, E., M. Arpin, A. Garcia, J. Finidori, and D. Louvard. 1986. A human villin cDNA to investigate the differentiation of the intestinal and kidney cells in vivo and in culture. *EMBO (Eur. Mol. Biol. Organ.) J.* 5:3119–3124.

Rana, A.P., P. Ruff, G.J. Maalouf, D.W. Speicher, and A.H. Chishti. 1993. Cloning of human erythroid dematin reveals another member of the villin family. *Proc. Natl. Acad. Sci. USA.* 90:6651–6655.

Riby, J.E., and N. Kretchmer. 1984. Effect of dietary sucrose on synthesis and degradation on intestinal sucrase. *Am. J. Physiol.* 246:G757–G763.

Robine, S., C. Huet, R. Moll, C. Sahuquillo-Merino, E. Coudrier, A. Zweibaum, and D. Louvard. 1985. Can villin be used to identify malignant and undifferentiated normal digestive epithelial cells? *Proc. Natl. Acad. Sci. USA.* 82:8488–8492.

Thomas, K.R., and M.R. Capecchi. 1987. Site-directed mutagenesis by gene targeting in mouse embryo-derived stem cell. *Cell.* 51:503–512.